Combustion Science and Technology, 1981, Vol. 25, pp. 159–174
0010-2202/81/2505-0159$06.50/0

A Monte Carlo Method for the PDF Equations of Turbulent Reactive Flow

S. B. POPE *Department of Mechanical Engineering, Massachusetts Institute of Technology, Cambridge, Massachusetts 02139*

(*Received September 25, 1980*)

Abstract—A Monte Carlo method is presented which simulates the transport equations of joint probability density functions (pdf's) in turbulent flows. (Finite-difference solutions of the equations are impracticable, mainly because of the large dimensionality of the pdf's). Attention is focused on an equation for the joint pdf of chemical and thermodynamic properties in turbulent reactive flows. It is shown that the Monte Carlo method provides a true simulation of this equation, and that the amount of computation required increases only linearly with the number of properties considered. Consequently, the method can be used to solve the pdf equation for turbulent flows involving many chemical species and complex reaction kinetics. Test calculations are reported that demonstrate the method and determine the influence of the numerical parameters. The method is then used to calculate pdf's of temperature in a turbulent mixing layer, and the calculations are found to be in good agreement with the measurements of Batt (1977). The method has previously been used to calculate the joint pdf of three reactive species in a premixed flame (Pope, 1981a).

1. INTRODUCTION

The closure problem associated with non-linearities in the equations governing turbulent flow is avoided by considering the joint probability density function (pdf) of the flow variables. The joint pdf of velocity $p(\mathbf{v}; \mathbf{x}, t)$ provides a complete statistical description of the turbulent velocity fluctuations, and, in reacting flows, a complete statistical description of the chemical and thermodynamic properties is provided by their joint pdf, $p(\boldsymbol{\psi}; \mathbf{x}, t)$.

These favorable attributes have led several authors to base turbulence closures on the transport equations for the joint pdf's. Lundgren (1969) and Ribeiro (1977) have suggested closure approximations for the transport equation for $p(\mathbf{v}; \mathbf{x}, t)$. For reacting flows, the transport equation for $p(\boldsymbol{\psi}; \mathbf{x}, t)$ is particularly attractive since the effects of reaction appear in closed form, irrespective of the complexity and non-linearity of the reaction scheme. Closure approximations for other terms in the equation have been suggested by Dopazo (1975), by Pope (1976) and by Janicka, Kolbe and Kollmann (1979). Recently, Pope (1981b) has studied the transport equation for the joint pdf $p(\mathbf{v}, \boldsymbol{\psi}; \mathbf{x}, t)$.

The attraction of the pdf approach appears to diminish when solving the transport equations is considered. Analytic solutions have been obtained in a few simple cases, but in general numerical methods are required. Such methods have to cope with the integro-differential nature of the equations and with the large dimensionality of $p(\mathbf{v}; \mathbf{x}, t)$ and $p(\boldsymbol{\psi}; \mathbf{x}, t)$. For example, in a steady, two-dimensional flow, the joint pdf of velocity is $p(v_1, v_2, v_3; x_1, x_2)$—a five-dimensional quantity. Consequently, no numerical solutions of the transport equation for $p(\mathbf{v}; \mathbf{x}, t)$ have been obtained. Janicka, Kolbe and Kollmann (1978) used a finite-difference method to solve the transport equation for a single scalar—that is, for $p(\psi; x_1, x_2)$. This is the most general solution that has been obtained so far.

Reactive flows of practical interest usually involve many species. Consequently the dimensionality of the pdf $p(\psi_1, \psi_2 \ldots \psi_\sigma; \mathbf{x}, t)$ is large because σ is large. An order-of-magnitude analysis (Section 3.6) shows that the finite-difference solution of the pdf transport equation is impracticable for σ greater than 3. (This is a generous estimate.) More importantly, the computational expense is found to rise exponentially with σ. Therefore no conceivable improvement in computational ability can make possible finite-difference solutions for $\sigma = 10$, say.

In this paper, a Monte Carlo method is presented which makes possible the solution of the pdf transport equation for the general case. The computational expense of the method rises only linearly with σ which is the best that can be achieved by any algorithm. Consequently, the solution of the pdf transport equation by the Monte Carlo method can be envisaged for turbulent flows involving many reactive species. Although it is specific to the

transport equation for $p(\psi; \mathbf{x}, t)$, the method contains the ingredients essential to simulating other joint pdf equations. Thus, solutions to the equations for $p(\mathbf{v}; \mathbf{x}, t)$ and $p(\mathbf{v}, \psi; \mathbf{x}, t)$ can be obtained.

In general, for simple problems Monte Carlo methods are inefficient compared with standard numerical techniques; but for multi-dimensional problems Monte Carlo methods remain practicable while other methods demand prohibitive amounts of computation. The works of Shreider (1966) and Handscomb and Hammersley (1965) describe various applications of the Monte Carlo method.

In the next section the transport equation for the joint pdf $p(\psi; \mathbf{x}, t)$ is presented and the modelling assumptions are discussed briefly. In Section 3 the Monte Carlo method is presented and analyzed to prove that it is a valid simulation of the pdf equation. Test calculations (reported in Section 4) demonstrate the method and are used to estimate its rate of convergence. The method was used to calculate pdf's of temperature in a turbulent mixing layer: the results, reported in Section 5, are in good agreement with the measurements of Batt (1977). In the final section the method is discussed starting with a summary of the more important findings.

2. THE JOINT PDF EQUATION

The equations presented here are taken from Pope (1979). A detailed description of the formulation and a discussion of the equations can be found in that work.

In a low Mach number flow, the mean pressure, the species concentrations and the enthalpy provide a complete description of the chemical and thermodynamic properties of the fluid at each point. Let $\phi_\alpha(\mathbf{x}, t)$ ($\alpha = 1, 2, \ldots \sigma$) denote one of the species mass fractions or the enthalpy at the location $\mathbf{x}$ and time t. Then, from conservation principles, the following equation for ϕ_α is obtained:

$$\rho\frac{\partial\phi_\alpha}{\partial t}+\rho U_i\frac{\partial\phi_\alpha}{\partial x_i}+\frac{\partial}{\partial x_i}J_i^\alpha = \rho S_\alpha. \qquad (2.1)$$

$U_i(\mathbf{x}, t)$ is the velocity in the x_i-direction; J_i^α is the flux of ϕ_α in the x_i-direction due to molecular transport; ρ is the density; and S_α is the rate of creation of ϕ_α. The set of quantities $\phi_1, \phi_2, \ldots, \phi_\sigma$ is denoted by $\boldsymbol{\varphi}$ and ρ and S_α can be expressed as functions of $\boldsymbol{\varphi}$: thus,

$$\rho = \rho(\boldsymbol{\varphi}) \quad \text{and} \quad S_\alpha = S_\alpha(\boldsymbol{\varphi}). \qquad (2.2)$$

The joint pdf of $\boldsymbol{\varphi}$ is $p(\psi; \mathbf{x}, t)$. ψ ($= \psi_1, \psi_2, \ldots, \psi_\sigma$) is the σ-dimensional composition space corresponding to $\boldsymbol{\varphi}$—a given location in composition space, $\boldsymbol{\varphi} = \boldsymbol{\psi}'$ say, corresponds to fluid of properties $\boldsymbol{\varphi} = \boldsymbol{\psi}'$. If $Q(\boldsymbol{\varphi})$ is any function of $\boldsymbol{\varphi}$ then its expected value (denoted by angled brackets) is

$$\langle Q(\boldsymbol{\varphi}(\mathbf{x}, t))\rangle = \int p(\psi; \mathbf{x}, t)\, Q(\psi)\, d\psi. \qquad (2.3)$$

$d\psi$ is written for $d\psi_1 d\psi_2 \ldots d\psi_\sigma$, indicating that integration is over the whole of ψ-space. In order to simplify the notation, $q(\mathbf{x}, t)$ will also be used for the expected value of Q:

$$q(\mathbf{x}, t) \equiv \langle Q(\boldsymbol{\varphi}(\mathbf{x}, t))\rangle. \qquad (2.4)$$

(The expected value of Q is sometimes called the ensemble average of Q: however, that term is reserved for a different use below.)

In variable-density flows the use of density-weighted averages has advantages both theoretically and practically. Density-weighted averages, denoted by a tilde, are defined by

$$\begin{aligned}\tilde{q}(\mathbf{x}, t) &\equiv \tilde{Q}(\boldsymbol{\varphi}(\mathbf{x}, t)) \\ &\equiv \langle \rho(\mathbf{x}, t)\, Q(\boldsymbol{\varphi}(\mathbf{x}, t))\rangle / \langle\rho\rangle. \end{aligned} \qquad (2.5)$$

And from the definition of the density-weighted joint pdf

$$\tilde{p}(\psi; \mathbf{x}, t) \equiv \rho(\psi) p(\psi; x, t)/\langle\rho\rangle \qquad (2.6)$$

it follows

$$\tilde{q}(\mathbf{x}, t) = \int \tilde{p}(\psi; \mathbf{x}, t)\, Q(\psi)\, d\psi. \qquad (2.7)$$

Henceforth, $\tilde{p}(\psi; \mathbf{x}, t)$ is written $\tilde{p}(\psi)$, the dependence upon $\mathbf{x}$ and t being implied.

A transport equation for $\tilde{p}(\psi)$ can be obtained from the conservation equation for ϕ_α, Eq. (2.1). If the turbulent transport is modelled by simple gradient diffusion (with the turbulent diffusion coefficient being $\Gamma_T(\mathbf{x}, t)$), the equation for $\tilde{p}(\psi)$ is

$$\begin{aligned}\frac{\partial\tilde{p}(\psi)}{\partial t}+\tilde{U}_i\frac{\partial\tilde{p}(\psi)}{\partial x_i}+\frac{\partial}{\partial\psi_\alpha}(\tilde{p}(\psi) S_\alpha(\psi)) \\ = \frac{1}{\langle\rho\rangle}\frac{\partial}{\partial x_i}\Gamma_T\frac{\partial\tilde{p}(\psi)}{\partial x_i}+E(\psi; \mathbf{x}, t). \end{aligned} \qquad (2.8)$$

Summation is over repeated indices (i and α) and $E(\psi; \mathbf{x}, t)$ represents the effect of molecular mixing. The terms on the left-hand side are exact whereas those on the right are modelled or (in the case E) need to be modelled. The two leading terms represent the rate of change of $\tilde{p}(\psi)$ along a density-

weighted streamline; the third term represents the transport of $\tilde{p}(\psi)$ in composition space due to reaction. It is noteworthy that, in this formulation, reaction—however complicated the scheme—can be treated without approximation.

Models for the molecular mixing term E have been proposed by Curl (1963), Dopazo (1975), Pope (1976) and Janicka *et al.* (1979), but none is entirely satisfactory. Here, Curl's model is employed since it alone is applicable to an arbitrary number of quantities (*i.e.*, any σ) and can be expected to produce qualitatively correct results. Accordingly, we take

$$E(\psi; \mathbf{x}, t) = 2^{\sigma}\omega \int \tilde{p}(\psi+\psi') \times \tilde{p}(\psi-\psi')d\psi' - \omega\tilde{p}(\psi) \quad (2.9)$$

where $\omega(\mathbf{x}, t)$ is the appropriate turbulent frequency. A more complete discussion of the modelling of the turbulent transport and of E is given by Pope (1979).

3. THE MONTE CARLO METHOD

The Monte Carlo method described in this section provides a simulation of the density-weighted joint pdf Eq. (2.8). The analysis presented here shows how the Monte Carlo method is devised and proves that it is a valid simulation. The usefulness of the method stems from the fact that the amount of computational work required increases only linearly with σ—the dimensionality of ψ.

3.1 *Dependent Variables*

The simulation is performed on a finite-difference grid, of uniform spacing h, which extends over the region of interest, $\mathbf{0} \leqslant \mathbf{x} \leqslant h\mathbf{L}$, say. The node denoted by $\mathbf{l}$ is located at $\mathbf{x} = \mathbf{l}h$. If $\mathbf{x}$-space is m-dimensional (in general $m = 3$), then $\mathbf{L}$ and $\mathbf{l}$ are m-vectors of integers and $0 \leqslant l_i \leqslant L_i$, $i = 1, 2, \ldots, m$. Each cycle of operations in the simulation advances time by an interval k. Hence, if initial conditions are supplied at $t = 0$, after λ cycles the time is $t = k\lambda$.

Rather than considering $\tilde{p}(\psi; \mathbf{x}, t)$ explicitly, the dependent variables in the simulation are *representative values of* φ. An *ensemble* of N such representative values is located at each grid node. The ensemble at $(\mathbf{x}, t) = (h\mathbf{l}, k\lambda)$ is denoted by $\Phi(h\mathbf{l}, k\lambda)$ and one of the N members of the ensemble is denoted by $\varphi^{(n)}(h\mathbf{l}, k\lambda)$. Although each member of the ensemble (or element) is ascribed a unique number, $1 \leqslant n \leqslant N$, no ordering is implied. In fact, operations are performed either on all members of the ensemble or on some selected at random. Thus, the numbering is a convenience that has no effect upon the outcome. Recalling that φ represents σ quantities, we may write the ensemble as,

$$\Phi(h\mathbf{l}, k\lambda) =$$
$$\varphi^{(1)}(h\mathbf{l}, k\lambda) = \phi_1^{(1)}, \phi_2^{(1)} \ldots \phi_\alpha^{(1)} \ldots \phi_\sigma^{(1)}$$
$$\varphi^{(2)}(h\mathbf{l}, k\lambda) = \phi_1^{(2)}, \phi_2^{(2)} \ldots \phi_\alpha^{(2)} \ldots \phi_\sigma^{(2)}$$
$$\vdots$$
$$\varphi^{(n)}(h\mathbf{l}, k\lambda) = \phi_1^{(n)}, \phi_2^{(n)} \ldots \phi_\alpha^{(n)} \ldots \phi_\sigma^{(n)}$$
$$\vdots$$
$$\varphi^{(N)}(h\mathbf{l}, k\lambda) = \phi_1^{(N)}, \phi_2^{(N)} \ldots \phi_\alpha^{(N)} \ldots \phi_\sigma^{(N)}.$$

The general element is $\varphi^{(n)}(h\mathbf{l}, k\lambda)$.

The *ensemble average* of any function $Q(\varphi)$ is defined by

$$\hat{q}(h\mathbf{l}, k\lambda) = Q(\Phi(h\mathbf{l}, k\lambda)) \equiv \frac{1}{N}\sum_{n=1}^{N} Q(\varphi^{(n)}(h\mathbf{l}, k\lambda)). \quad (3.1)$$

The ensemble average $\hat{q}$ is intended to simulate the density-weighted average $\tilde{q}$.

3.2 *Initial Conditions*

In most applications the initial conditions are likely to be simple—a uniform composition for example. Consequently the task of specifying the initial ensembles is also likely to be simple. However, a consideration of the general case is informative.

At the node $h\mathbf{l}$, the initial values of the elements are chosen to be

$$\varphi^{(n)}(h\mathbf{l}, 0) = \xi^{(n)}. \quad (3.2)$$

$\xi^{(n)}$ is the value (on the nth trial) of a random vector ξ which is distributed identically to $\varphi(h\mathbf{l}, 0)$ —that is,

$$p(\xi)d\xi = \tilde{p}(\psi; h\mathbf{l}, 0)d\psi. \quad (3.3)$$

For any function $Q(\psi)$, the expected value of

$Q(\boldsymbol{\varphi}^{(n)})$ is

$$\mathsf{E}Q(\boldsymbol{\varphi}^{(n)}(h\mathbf{l}, 0)) = \int Q(\xi)p(\xi)d\xi$$
$$= \int Q(\boldsymbol{\psi})\tilde{p}(\boldsymbol{\psi}; h\mathbf{l}, 0)d\boldsymbol{\psi}$$
$$= \tilde{q}(h\mathbf{l}, 0). \tag{3.4}$$

It clearly follows that the expected value of the ensemble average of Q is also $\tilde{q}$:

$$\mathsf{E}\hat{q}(h\mathbf{l}, 0) = \tilde{q}(h\mathbf{l}, 0). \tag{3.5}$$

The above shows that $\hat{q}(h\mathbf{l}, 0)$ is an unbiased estimate of $\tilde{q}(h\mathbf{l}, 0)$. The error in this estimate can be determined from the Central Limit Theorem (Gnedenko, 1962): since $\hat{q}$ is the average of N independent random samples,

$$Q(\boldsymbol{\varphi}^{(n)}(h\mathbf{l}, 0)), \qquad n = 1, 2 \ldots N,$$

as N tends to infinity the inequality

$$|\hat{q}(h\mathbf{l}, 0) - \tilde{q}(h\mathbf{l}, 0)| < \beta q' N^{-1/2} \tag{3.6}$$

holds with probability $\mathrm{erf}(\beta/\sqrt{2})$, for $\beta > 0$. q' is the standard deviation

$$(q')^2 = \mathsf{D}Q(\boldsymbol{\varphi}) = \int \tilde{p}(\boldsymbol{\psi})(Q(\boldsymbol{\psi}) - \tilde{q})^2 d\boldsymbol{\psi}. \tag{3.7}$$

Thus in the limit of large N, $\hat{q}$ (determined from Φ) converges in probability to $\tilde{q}$ (determined from $\tilde{p}(\boldsymbol{\psi})$) for any function $Q(\boldsymbol{\psi})$.

These considerations lead to the definition of *equivalence* which is used extensively in the subsequent analysis. If for all functions Q, the ensemble average $\hat{q}(h\mathbf{l}, t)$ converges in probability to the expected value $\tilde{q}(h\mathbf{l}, t)$, then $\Phi(h\mathbf{l}, t)$ and $\tilde{p}(\boldsymbol{\psi}; h\mathbf{l}, t)$ are equivalent. Equivalence is denoted by an arrow:

$$\Phi(h\mathbf{l}, t) \to \tilde{p}(\boldsymbol{\psi}; h\mathbf{l}, t)$$

or

$$\hat{q}(h\mathbf{l}, t) \to \tilde{q}(h\mathbf{l}, t).$$

Clearly, the initial ensembles are equivalent to the initial pdf's.

3.3 *Outline of the Analysis*

The analysis proceeds in two stages. First a finite-difference scheme is constructed in physical space and time (but not in composition space). From the initial condition $\tilde{p}(\boldsymbol{\psi}; h\mathbf{l}, 0)$, after λ time steps of duration k, the finite-difference scheme yields the solution $\tilde{p}_{fd}(\boldsymbol{\psi}; h\mathbf{l}, k\lambda)$ where:

$$\tilde{p}_{fd}(\boldsymbol{\psi}; h\mathbf{l}, k\lambda) = \tilde{p}(\boldsymbol{\psi}; h\mathbf{l}, k\lambda) + 0(k, h). \tag{3.8}$$

The grid spacing h and time step k are to be chosen so that the truncation error is less than the required tolerance.

A Monte Carlo method is then devised to simulate the finite-difference solution. The simulation starts with the initial ensembles $\Phi(h\mathbf{l}, 0)$ being equivalent to the initial pdf's $\tilde{p}(\boldsymbol{\psi}; h\mathbf{l}, 0)$. Then, at successive time steps, the ensembles are altered in such a way that they remain equivalent to $\tilde{p}_{fd}(h\mathbf{l}, \lambda k)$. The ensembles change both by shifting elements from node to node (simulating transport in physical space) and by changing the values of $\boldsymbol{\varphi}^{(n)}$ (simulating transport in composition space). Thus, after λ steps the ensembles $\Phi(h\mathbf{l}, \lambda k)$ are equivalent to the joint pdf's $\tilde{p}_{fd}(\boldsymbol{\psi}; h\mathbf{l}, \lambda k)$ which, to within truncation error, are equal to $\tilde{p}(\boldsymbol{\psi}; h\mathbf{l}, \lambda k)$ —the solution to Eq. (2.8).

The finite-difference scheme is constructed in the next sub-section and the Monte Carlo simulation is presented in 3.5.

3.4 *Finite-Difference Scheme*

Equation (2.8) shows that $\tilde{p}(\boldsymbol{\psi}; \mathbf{x}, t)$ changes due to the simultaneous action of convection, reaction, diffusion and mixing. These four processes can be treated sequentially by using the technique of operator splitting. Hence the following operators are defined:

$$\boldsymbol{C}_{(i)} \equiv \tilde{U}_{(i)} \frac{\partial}{\partial x_{(i)}}, \tag{3.9}$$

$$\boldsymbol{S} \equiv S_\alpha(\boldsymbol{\psi}) \frac{\partial}{\partial \psi_\alpha} + \left(\frac{\partial S_\alpha}{\partial \psi_\alpha}\right)\boldsymbol{I}, \tag{3.10}$$

and

$$\boldsymbol{D}_{(i)} \equiv \frac{1}{\langle \rho \rangle} \frac{\partial}{\partial x_{(i)}} \Gamma_T \frac{\partial}{\partial x_{(i)}}. \tag{3.11}$$

$\boldsymbol{I}$ is the identity operator and the summation convention is suspended for bracketed suffices. The operator $\boldsymbol{E}$ is defined by

$$\boldsymbol{E}\tilde{p}(\boldsymbol{\psi}; \mathbf{x}, t) \equiv E(\boldsymbol{\psi}; \mathbf{x}, t), \tag{3.12}$$

E being given by Eq. (2.9). For an m-dimensional flow (in general $m = 3$) the transport equation for $\tilde{p}$ can be written,

$$\frac{\partial \tilde{p}(\boldsymbol{\psi})}{\partial t} = \left\{\boldsymbol{E} - \boldsymbol{S} - \sum_{i=1}^{m} \boldsymbol{C}_{(i)} + \sum_{j=1}^{m} \boldsymbol{D}_{(j)}\right\}\tilde{p}(\boldsymbol{\psi}). \tag{3.13}$$

By approximating the time derivative by the forward difference

$$\frac{1}{k}(\tilde{p}(\boldsymbol{\psi}; \mathbf{x}, t+k)-\tilde{p}(\boldsymbol{\psi}; \mathbf{x}, t)) = \frac{\partial \tilde{p}(\boldsymbol{\psi}; \mathbf{x}, t)}{\partial t}+\boldsymbol{0}(k) \tag{3.14}$$

we obtain

$$\tilde{p}(\boldsymbol{\psi}; \mathbf{x}, t+k) = \left\{\boldsymbol{I}+k\boldsymbol{E}-k\boldsymbol{S}-k\sum_{i=1}^{m}\boldsymbol{C}_{(i)}+k\sum_{j=1}^{m}\boldsymbol{D}_{(j)}\right\} \times \tilde{p}(\boldsymbol{\psi}; \mathbf{x}, t)+\boldsymbol{0}(k^2). \tag{3.15}$$

The spatial differential operators $\boldsymbol{D}$ and $\boldsymbol{C}$ are replaced by the finite-difference operators $\boldsymbol{D}^*$ and $\boldsymbol{C}^*$. The second-order-accurate central difference is used for $\boldsymbol{D}^*$,

$$\begin{aligned}\boldsymbol{D}_{(i)}{}^*f(\mathbf{x}) &\equiv \{\Gamma_T(\mathbf{x}+\tfrac{1}{2}e_i h)[f(\mathbf{x}+e_i h)-f(\mathbf{x})] \\ &\quad -\Gamma_T(\mathbf{x}-\tfrac{1}{2}e_i h) \\ &\quad \times[f(\mathbf{x})-f(\mathbf{x}-e_i h)]\}/(\langle\rho\rangle)h^2) \\ &= \boldsymbol{D}_{(i)}f(\mathbf{x})+\boldsymbol{0}(h^2)\end{aligned} \tag{3.16}$$

where $\mathbf{e}$ is the unit vector. The first-order-accurate upwind difference is used for $\boldsymbol{C}_{(i)}{}^*$,

$$\begin{aligned}\boldsymbol{C}_{(i)}{}^*f(\mathbf{x}) &\equiv |\tilde{U}_{(i)}(\mathbf{x})|\{f(\mathbf{x})-f(\mathbf{x}-e_i' h)\}/h \\ &= \boldsymbol{C}_{(i)}f(\mathbf{x})+\boldsymbol{0}(h)\end{aligned} \tag{3.17}$$

where e_i' is the unit vector in the same direction as $\tilde{U}_i$, *i.e.*

$$\begin{aligned} e_i' &= e_i, \qquad \tilde{U}_i \geqslant \boldsymbol{0} \\ e_i' &= -e_i, \qquad \tilde{U}_i < \boldsymbol{0}\end{aligned} \tag{3.18}$$

With $\boldsymbol{D}^*$ and $\boldsymbol{C}^*$ replacing $\boldsymbol{D}$ and $\boldsymbol{C}$, Eq. (3.15) becomes,

$$\tilde{p}(\boldsymbol{\psi}; \mathbf{x}, t+k) = \left\{\boldsymbol{I}+k\boldsymbol{E}-k\boldsymbol{S}-k\sum_{i=1}^{m}\boldsymbol{C}_{(i)}{}^*+k\sum_{j=1}^{m}\boldsymbol{D}_{(j)}{}^*\right\} \times\tilde{p}(\boldsymbol{\psi}; \mathbf{x}, t)+k\boldsymbol{0}(h, k). \tag{3.19}$$

In the above equation, the term in braces is the sum of operators which can be factored into products of operators plus terms of order k^2. For example, the first three operators can be factored as,

$$\begin{aligned}(\boldsymbol{I}+k\boldsymbol{E}-k\boldsymbol{S}) &= (\boldsymbol{I}+k\boldsymbol{E})(\boldsymbol{I}-k\boldsymbol{S})+k^2\boldsymbol{E}\boldsymbol{S} \\ &= (\boldsymbol{I}+k\boldsymbol{E})(\boldsymbol{I}-k\boldsymbol{S})+\boldsymbol{0}(k^2).\end{aligned} \tag{3.20}$$

The sum of operators in Eq. (3.19) is factored similarly to produce,

$$\begin{aligned}\tilde{p}(\boldsymbol{\psi}; \mathbf{x}, t+k) &= (\boldsymbol{I}+k\boldsymbol{E})(\boldsymbol{I}-k\boldsymbol{S})\prod_{i=1}^{m}(\boldsymbol{I}-k\boldsymbol{C}_{(i)}{}^*) \\ &\quad \times\prod_{j=1}^{m}(\boldsymbol{I}+k\boldsymbol{D}_{(j)}{}^*)\tilde{p}(\boldsymbol{\psi}; \mathbf{x}, t) \\ &\quad +k\boldsymbol{0}(h, k).\end{aligned} \tag{3.21}$$

The operator product that acts on $\tilde{p}(\boldsymbol{\psi}; \mathbf{x}, t)$ can be split into a sequence of operators acting on the intermediate values $\tilde{p}(\boldsymbol{\psi}; \mathbf{x}, t')$, where $t \leqslant t' < t+k$. (This is a device that aids the notation: t' is not intended to correspond to any particular time.) The notional times $t_{d(i)}$ and $t_{c(i)}$ refer to the pdf's after diffusion and convection in the x_i-direction. After reaction and mixing the notional times are t_r and t_m. These times are related by

$$\begin{aligned} t &= t_{d(0)} < t_{d(1)} \ldots < t_{d(m)} \\ &= t_{c(0)} < t_{c(1)} \ldots < t_r < t_m < t+k.\end{aligned}$$

(This relation also defines $t_{d(0)}$ and $t_{c(0)}$.) In terms of these intermediate times, at $\mathbf{x} = h\mathbf{l}$, the sequence of operation is

$$\tilde{p}(\boldsymbol{\psi}; h\mathbf{l}, t_{d(i)}) = (\boldsymbol{I}+k\boldsymbol{D}_{(i)}{}^*)\tilde{p}(\boldsymbol{\psi}; h\mathbf{l}, t_{d(i-1)}), \quad i = 1, \ldots, m, \tag{3.22}$$

$$\tilde{p}(\boldsymbol{\psi}; h\mathbf{l}, t_{c(i)}) = (\boldsymbol{I}-k\boldsymbol{C}_{(i)}{}^*)\tilde{p}(\boldsymbol{\psi}; h\mathbf{l}, t_{c(i-1)}), \quad i = 1, \ldots, m, \tag{3.23}$$

$$\tilde{p}(\boldsymbol{\psi}; h\mathbf{l}, t_r) = (\boldsymbol{I}-k\boldsymbol{S})\tilde{p}(\boldsymbol{\psi}; h\mathbf{l}, t_{c(m)}), \tag{3.24}$$

$$\tilde{p}(\boldsymbol{\psi}; h\mathbf{l}, t_m) = (\boldsymbol{I}+k\boldsymbol{E})\tilde{p}(\boldsymbol{\psi}; h\mathbf{l}, t_r), \tag{3.25}$$

The value of $\tilde{p}$ after the mixing operation is an approximation to $\tilde{p}(\boldsymbol{\psi}; \mathbf{x}, t+k)$, and according to Eq. (3.21)

$$\tilde{p}(\boldsymbol{\psi}; h\mathbf{l}, t+k) = \tilde{p}(\boldsymbol{\psi}; h\mathbf{l}, t_m)+k\boldsymbol{0}(h, k) \tag{3.26}$$

Equations (3.22–3.26) define the finite-difference scheme. It is fully explicit and first-order accurate in both space and time. Such schemes for convective–diffusive equations are known to be stable

conditional on the time-step restrictions

$$\Gamma_T k/h^2 < \tfrac{1}{2}, \tag{3.27}$$

and

$$|\tilde{U}|k/h < 1. \tag{3.28}$$

3.5 *Monte Carlo Simulation*

A Monte Carlo method is devised to simulate the finite-difference solution of the pdf transport equation. At each grid node the pdf is represented by an ensemble of N elements. These ensembles are modified at each time step so as to simulate each of the four processes—diffusion, convection, reaction and mixing. For the finite-difference scheme, the effect that each process has upon $\tilde{q}$ can be determined by multiplying Eqs. (3.22–3.25) by $Q(\boldsymbol{\psi})$ and integrating. The Monte Carlo simulations are constructed so that the effects upon $\hat{q}$ are the same. To be more precise, let t' and t'' be the notional times before and after a particular process, and let the ensemble and pdf be equivalent at t':

$$\hat{q}(h\mathbf{l}, t') \to \tilde{q}(h\mathbf{l}, t'). \tag{3.29}$$

We seek a simulation of the process such that

$$\hat{q}(h\mathbf{l}, t'') \to \tilde{q}(h\mathbf{l}, t''), \tag{3.30}$$

for all $Q(\boldsymbol{\psi})$. This condition is sufficient to ensure that as N tends to infinity the ensemble $\Phi(h\mathbf{l}, t+k)$ converges to the pdf $\tilde{p}(\boldsymbol{\psi}; h\mathbf{l}, t+k)$ obtained from the finite-difference scheme. Hence, as h and k tend to zero, the Monte Carlo method provides a true simulation of the pdf transport Eq. (2.8).

Diffusion The effect upon $\tilde{q}$ of diffusion in the x_i-direction is determined by multiplying Eq. (3.22) by $Q(\boldsymbol{\psi})$ and integrating:

$$\tilde{q}(h\mathbf{l}, t_{d(i)}) = (\boldsymbol{I}+k\boldsymbol{D}_{(i)}{}^*)\tilde{q}(h\mathbf{l}) \tag{3.31}$$

$$= (1-\gamma_{i+}-\gamma_{i-})\tilde{q}(h\mathbf{l})+\gamma_{i+}\tilde{q}(h(\mathbf{l}+e_{(i)})) + \gamma_{i-}\tilde{q}(h(\mathbf{l}-e_{(i)})), \tag{3.32}$$

where the Fourier numbers γ are

$$\gamma_{i\pm} = \frac{k}{h^2}\frac{1}{\langle\rho\rangle}\Gamma_T(h(\mathbf{l}\pm\tfrac{1}{2}e_i), k\lambda). \tag{3.33}$$

(Here, and below, $\tilde{q}(h\mathbf{l})$ refers to the value before the process, *i.e.* to $\tilde{q}(h\mathbf{l}, t_{d(i-1)})$.) Thus, $\tilde{q}(h\mathbf{l}, t_{d(i)})$ is a weighted average of $\hat{q}(h\mathbf{l})$ and the values at the two neighbouring nodes $\tilde{q}(h(\mathbf{l}\pm e_i))$.

This process is simulated by forming $\Phi(h\mathbf{l}, t_{d(i)})$ from elements selected at random from $\Phi(h\mathbf{l})$ and $\Phi(h(\mathbf{l}\pm e_i))$ in appropriate proportions. The numbers of elements selected from $\Phi(h(\mathbf{l}\pm e_i))$ are $n_{di\pm}$, the nearest integers to

$$n_{di\pm}{}' = N\gamma_{i\pm} \tag{3.34}$$

and the remaining n_{di} $(=N-n_{di+}-n_{di-})$ elements are selected from $\Phi(h\mathbf{l})$. Thus, with $\boldsymbol{\varphi}^*$ denoting an element selected at random without replacement, the ensemble average after diffusion is

$$\hat{q}(h\mathbf{l}, t_{d(i)}) = \frac{1}{N}\sum_{n_{di+}} Q\{\boldsymbol{\varphi}^*[h(\mathbf{l}+e_{(i)})]\} + \frac{1}{N}\sum_{n_{di-}} Q\{\boldsymbol{\varphi}^*[h(\mathbf{l}-e_{(i)})]\} + \frac{1}{N}\sum_{n_{di}} Q\{\boldsymbol{\varphi}^*(h\mathbf{l})\}. \tag{3.35}$$

The expected value of the last term is

$$\mathsf{E}\frac{1}{N}\sum_{n_{di}} Q(\boldsymbol{\varphi}^*(h\mathbf{l})) = \frac{n_{di}}{N}\,\mathsf{E}\frac{1}{n_{di}}\sum_{n_{di}} Q(\boldsymbol{\varphi}^*(h\mathbf{l})) = (1-\gamma_{i+}-\gamma_{i-})\hat{q}(h\mathbf{l}). \tag{3.36}$$

Applying the same procedure to the other terms yields

$$\mathsf{E}\hat{q}(h\mathbf{l}, t_{d(i)}) = (1-\gamma_{i+}-\gamma_{i-})\hat{q}(h\mathbf{l}) + \gamma_{i+}\hat{q}(h(\mathbf{l}+e_{(i)})) + \gamma_{i-}\hat{q}(h(\mathbf{l}-e_{(i)})). \tag{3.37}$$

As N tends to infinity $\hat{q}(h\mathbf{l}, t_{d(i)})$ converges to its expected value. Thus, if $\hat{q} \to \tilde{q}$ prior to diffusion, a comparison of Eqs. (3.32) and (3.37) reveals that

$$\hat{q}(h\mathbf{l}, t_{d(i)}) \to \tilde{q}(h\mathbf{l}, t_{d(i)}). \tag{3.38}$$

This result confirms that the simulation of diffusion is valid (*cf.* Eq. 3.30)).

An efficient implementation of the simulation of diffusion is the following. Each line of nodes in the x_i-direction is taken in turn. At each node along the line, groups of n_{di+} and n_{di-} elements are selected at random without replacement from the ensemble. The group of n_{di+} elements at $h\mathbf{l}$ is then commuted with the group of n_{di-} elements at $h(\mathbf{l}+e_i)$. (From the definition of $n_{di\pm}$ it may be seen that the sizes of these groups are the same.) This process is performed for each node along the line and for each line of nodes. The resulting ensembles are $\Phi(h\mathbf{l}, t_{d(i)})$.

Convection The development of a simulation of convection is similar to that for diffusion. Multiplying Eq. (3.23) by $Q(\psi)$ and integrating shows the effect of convection in the x_i-direction to be

$$\begin{aligned}\tilde{q}(h\mathbf{l}, t_{c(i)}) &= (\boldsymbol{I}-k\boldsymbol{C}_{(i)}{}^{*})\tilde{q}(h\mathbf{l}) \\ &= (1-c_i)\tilde{q}(h\mathbf{l})+c_i\tilde{q}(h\mathbf{l}-e_{(i)}'), \quad (3.39)\end{aligned}$$

where the Courant number c_i is

$$c_i = \frac{k}{h}|\tilde{U}_i(h\mathbf{l}, k\lambda)|. \quad (3.40)$$

Thus, $\tilde{q}(h\mathbf{l}, t_{c(i)})$ is the weighted average of $\tilde{q}(h\mathbf{l})$ and the value at the upwind node $\tilde{q}(h(\mathbf{l}-e_i'))$.

Convection is simulated along each line of nodes in the x_i-direction taken in turn. At each node, n_{ci} elements selected at random are replaced by n_{ci} elements selected at random from the upstream node. The resulting ensembles are $\Phi(h\mathbf{l}, t_{c(i)})$. The number n_{ci} is the nearest integer to

$$n_{ci}' = Nc_i \quad (3.47)$$

By arguments similar to those employed for the diffusive process, it can readily be shown that, if $\hat{q} \to \tilde{q}$, then

$$\hat{q}(h\mathbf{l}, t_{c(i)}) \to \tilde{q}(h\mathbf{l}, t_{c(i)}). \quad (3.42)$$

This confirms the validity of the simulation of convection.

Reaction Both convection and diffusion transport $\tilde{p}(\psi; \mathbf{x}, t)$ in $\mathbf{x}$-space. Consequently they are both simulated by the transfer of elements from one node to another. Reaction and mixing, on the other hand, transport $\tilde{p}(\psi; \mathbf{x}, t)$ in ψ-space. This is simulated by changing the composition of elements at each node. Of the four processes, only reaction is simulated deterministically.

The effect of reaction upon $\tilde{q}$ is determined by multiplying Eq. (3.24) by $Q(\psi)$ and integrating. At $\mathbf{x} = h\mathbf{l}$ this gives:

$$\tilde{q}(h\mathbf{l}, t_r) = \tilde{q}(h\mathbf{l}, t_{c(m)})+k\tilde{r}(h\mathbf{l}, t_{c(m)}) \quad (3.43)$$

where $\tilde{r}$ is the expected value of $R(\varphi)$,

$$R(\varphi) = S_\alpha(\varphi)\frac{\partial Q(\varphi)}{\partial \phi_\alpha}. \quad (3.44)$$

For each element $\varphi^{(n)} = \varphi^{(n)}(h\mathbf{l}, t_{c(m)})$ reaction proceeds according to

$$\varphi^{(n)}(h\mathbf{l}, t_r) = \varphi^{(n)}+\Delta\varphi^{(n)}, \quad (3.45)$$

where the undetermined quantity $\Delta\varphi^{(n)}$ is of order k. The effect of reaction upon $\hat{q}$ is determined from Eq. (3.45) by use of a Taylor expansion:

$$\begin{aligned}&\hat{q}(h\mathbf{l}, t_r) \\ &= \frac{1}{N}\sum_{n=1}^{N} Q(\varphi^{(n)}+\Delta\varphi^{(n)}) \\ &= \frac{1}{N}\sum_{n=1}^{N}\left\{Q(\varphi^{(n)})+\Delta\phi_\alpha{}^{(n)}\frac{\partial Q(\varphi^{(n)})}{\partial \phi_\alpha{}^{(n)}}+0(k^2)\right\}.\end{aligned} \quad (3.46)$$

The appropriate choice for $\Delta\phi^{(n)}$ is

$$\Delta\phi_\alpha{}^{(n)} = kS_\alpha(\varphi^{(n)})+0(k^2), \quad (3.47)$$

since Eq. (3.46) then becomes

$$\begin{aligned}\hat{q}(h\mathbf{l}, t_r) &= \hat{q}(h\mathbf{l}, t_{c(m)}) \\ &\quad +k\hat{r}(h\mathbf{l}, t_{c(m)})+0(k^2), \quad (3.48)\end{aligned}$$

where $\hat{r}$ is the ensemble average of R. And a comparison of Eqs. (3.43) and (3.48) shows that, if $\hat{q} \to \tilde{q}$ prior to reaction, then the required result is obtained, namely:

$$\hat{q}(h\mathbf{l}, t_r) \to \tilde{q}(h\mathbf{l}, t_r)+0(k^2). \quad (3.49)$$

(The truncation error $0(k^2)$ is of the same order as that in the finite-difference scheme and hence is of no concern in this analysis. In fact, no truncation error results from the simulation of reaction, see Section 3.6.)

A physical interpretation of the reaction process is simply that each element reacts independently for an interval of time k according to the ordinary differential equations

$$\frac{d\phi_\alpha{}^{(n)}}{dt} = S_\alpha(\varphi^{(n)}), \qquad \alpha = 1, 2, \ldots, \sigma. \quad (3.50)$$

The resulting change in $\varphi^{(n)}$ is in accord with Eq. (3.47). The implementation of reaction is discussed further in Section 3.6.

Mixing The effect of mixing upon $\tilde{q}$ is determined by multiplying Eq. (3.25) by $Q(\psi)$ and integrating. The result is

$$\tilde{q}(h\mathbf{l}, t_m) = (1-\omega k)\tilde{q}(h\mathbf{l}, t_r)+\omega k v(h\mathbf{l}, t_r), \quad (3.51)$$

where,

$$v = \int\tilde{p}(\psi')\int\tilde{p}(\psi)\,Q(\tfrac{1}{2}(\psi+\psi'))\,d\psi\,d\psi'. \quad (3.52)$$

In the simulation, $\Phi(h\mathbf{l}, t_m)$ is composed of $N-n_m$ elements selected at random from $\Phi(h\mathbf{l}, t_r)$ with the remaining n_m elements being "mixed". The number n_m is the integer nearest to

$$n_m' = N\omega k.$$

The elements from $\Phi(h\mathbf{l}, t_r)$ simulate the first term on the right-hand side of Eq. (3.51): the composition of the "mixed" elements should be such that they account for the second term. This composition is determined by simulating the double integral v. If $\hat{q}(t_r) \to \tilde{q}(t_r)$, then for the inner integral of Eq. (3.52),

$$\int \tilde{p}(\boldsymbol{\psi})\, Q(\tfrac{1}{2}(\boldsymbol{\psi}+\boldsymbol{\psi}'))\, d\boldsymbol{\psi} \to \frac{1}{N}\sum_{n=1}^{N} Q(\tfrac{1}{2}(\boldsymbol{\varphi}^{(n)}+\boldsymbol{\psi}')). \tag{3.53}$$

Thus, for the outer integral,

$$v \to \int \frac{1}{N}\sum_{n=1}^{N} Q(\tfrac{1}{2}(\boldsymbol{\varphi}^{(n)}+\boldsymbol{\psi}'))\tilde{p}(\boldsymbol{\psi}')\, d\boldsymbol{\psi}' \to \frac{1}{N}\sum_{n=1}^{N}\frac{1}{N}\sum_{n'=1}^{N} Q(\tfrac{1}{2}(\boldsymbol{\varphi}^{(n)}+\boldsymbol{\varphi}^{(n')})). \tag{3.54}$$

In the above equation, $\frac{1}{2}(\boldsymbol{\varphi}^{(n)}+\boldsymbol{\varphi}^{(n')})$ is the average value of the composition of two elements, and the summation is over all N^2 pairs of elements. The same result is obtained if a random sample of size n_m is used:

$$v \to \frac{1}{n_m}\sum_{n_m} Q(\boldsymbol{\varphi}^{\mathrm{mix}}), \tag{3.55}$$

where each value of $\boldsymbol{\varphi}^{\mathrm{mix}}$ is the average composition of a pair of elements selected at random *with* replacement from $\Phi(h\mathbf{l}, t_r)$.

In summary, $n_m \approx N\omega k$ mixed elements are formed from $\Phi(t_r)$: these are then used to replace n_m elements selected at random from $\Phi(t_r)$. The resulting ensemble is $\Phi(t_m)$.

With $\boldsymbol{\varphi}^*$ denoting an element selected at random without replacement from $\Phi(h\mathbf{l}, t_r)$, the ensemble average $\hat{q}(h\mathbf{l}, t_m)$ is

$$\hat{q}(h\mathbf{l}, t_m) = \frac{1}{N}\sum_{N-n_m} Q(\boldsymbol{\varphi}^*) + \frac{1}{N}\sum_{n_m} Q(\boldsymbol{\varphi}^{\mathrm{mix}}). \tag{3.56}$$

If $\hat{q}(t_r) \to \hat{q}(t_m)$ then from (3.51), (3.55), (3.56) and the definition of n_m

$$\hat{q}(h\mathbf{l}, t_m) \to (1-\omega k)\tilde{q}(h\mathbf{l}, t_r) + \omega k\, v(h\mathbf{l}, t_r) \to \tilde{q}(h\mathbf{l}, t_m), \tag{3.57}$$

which is the required result.

Summary In Section 3.4 a finite-difference scheme was obtained (Eqs. 3.22–3.26) for the transport equation of $\tilde{p}(\boldsymbol{\psi}; \mathbf{x}, t)$, Eq. (2.8). For each of the four processes—diffusion, convection, reaction and mixing—a Monte Carlo simulation has now been obtained. Each simulated process has been shown to be valid since the ensembles and pdf's remain equivalent through the process. Thus, to within truncation error, ensemble averages obtained from the Monte Carlo simulation are equal to density-weighted averages obtained from the solution to Eq. (2.8).

The simulations of diffusion and convection can be performed only for the time step k being less than some limit, since otherwise samples of a size greater than N are called for. The restrictions imposed by diffusion and convection are

$$(n_{di+}+n_{di-}) \leqslant N, \tag{3.58}$$

and

$$n_{ci} \leqslant N. \tag{3.59}$$

The resulting restrictions on k are exactly the same as the conditional stability limits of the finite-difference scheme, Eqs. (3.27) and (3.28). These time-step restrictions are of no consequence since (it is shown in the next section) the computational effort required per step is proportional to k. Hence a small value of k can be chosen (with a consequent gain in accurary) without any penalty in computational expense.

Since the scheme is explicit, the specification of boundary conditions is straightforwad.

3.6 *Computational Efficiency*

The computational efficiency of the Monte Carlo method depends upon the computer work W and the numerical error ϵ involved in performing the simulation for a time $T = \lambda k$. In this section it is shown that the computer work is proportional to $N\sigma T$. This result is important for two reasons. That the work rises only linearly with σ (the dimensionality of $\boldsymbol{\psi}$-space) shows that the method is practicable for large σ. (This is in marked contrast to a finite-difference scheme for which the work is estimated to rise as $e^{a\sigma}$, $a \approx 6$.) The second

significance of the result is that the computer work is independent of the time step size k. Consequently there is no penalty in choosing a small time step and hence virtually eliminating the associated truncation error.

The error in the simulation is due to both truncation and sampling error. As N tends to infinity, the sampling error tends to zero, thus isolating the truncation error. This—according to Eq. (3.26)—is of order k and h, and hence the scheme is first-order accurate in space and time. The sampling error caused by a finite value of N is more difficult to determine. An error analysis reported elsewhere (Pope, 1980) and the test calculations of the next section suggest that the sampling error is of order $N^{-1/2}$ and independent of σ and h. With these estimates of the computer work W and the numerical error ϵ, for a given grid (fixed h), we obtain

$$W \propto \sigma T/\epsilon^2 \tag{3.60}$$

Thus the work is linearly proportional to σ and T (the best that can be achieved) but, in common with all Monte Carlo methods, the rate of convergence is slow: four times the amount of work only halves the error.

The dependence of the work upon σ, N and k is now determined assuming h and m to be fixed.

Interestingly, both the diffusion and convection processes involve no arithmetic, only data manipulation. Of order n_{di} or n_{ci} elements are involved and the number of operations per element is proportional to σ. Since n_{di} and n_{ci} are of order kN, the number of operations per node per time step is of order $kN\sigma$. A similar argument leads to the same result for the mixing operation. Thus, for these three processes, in order to take λ steps ($\lambda = T/k$), of order $kN\sigma\lambda = N\sigma T$ operations are required.

The implementation of reaction as described in Section 3.5 is not computationally efficient. An efficient algorithm exploits the fact that, between mixing operations, only reaction affects the composition of an element. If a given element has not been involved in mixing for λ_r steps, then its composition can be obtained by integrating the equations

$$\frac{d\phi_\alpha}{dt} = S_\alpha(\boldsymbol{\varphi}) \qquad \alpha = 1, 2, \ldots, \sigma, \tag{3.61}$$

for a time $\tau = k\lambda_r$, taking the composition after the last mixing as the initial condition. Thus, rather than integrating Eqs. (3.61) for all N elements for an interval k, the efficient algorithm integrates the equations for the n_m elements involved in mixing for the longer intervals τ. The average value of τ is ω^{-1}, independent of k.

The amount of work required by this algorithm depends upon the complexity of the reaction scheme. If the reaction scheme is fairly simple it can be assumed that the computer time required to integrate Eqs. (3.61) is proportional to the number of equations, *i.e.* proportional to σ. Then, the total work required to simulate reaction is proportional to $N\sigma T$.

It has now been shown that for each of the four processes, and hence for the scheme as a whole, that the amount of computer work is proportional to $N\sigma T$ and independent of k.

By comparison, the number of computer operations required by a straightforward finite-difference scheme increases exponentially with σ. If $\boldsymbol{\psi}$-space is discretized into, say, 20 divisions in each direction, then the number of nodes in the space is $(20)^\sigma$. The double integral in Eq. (2.9) requires the evaluation of a volume integral in $\boldsymbol{\psi}$-space for each $\boldsymbol{\psi}$-node: this requires of order $(20)^{2\sigma}$ operations. Thus, at each node in $\boldsymbol{\psi}$-space, for each time step, of order $(20)^{2\sigma} \approx e^{6\sigma}$ operations are required. The values shown in Table I may be compared with current computation rates of order 10^6 s^{-1}.

If not impracticable, solutions for $\sigma = 3$ would be very expensive. For $\sigma = 4$, finite-difference solutions are definitely impracticable. The main point to note, however, is that the number of operations increases exponentially with σ. As long as this is so, no conceivable refinement to the finite-difference scheme or improvement in computing speed can facilitate solutions for large σ.

TABLE I
Computer operations required by a finite-difference scheme, per node per time step

Dimensionality of the joint pdf σ	Approximate number of operations required by finite-difference scheme $e^{6\sigma}$
1	4.0×10^2
2	1.6×10^5
3	6.6×10^7
4	2.6×10^{10}
5	1.1×10^{13}

4. TEST CALCULATIONS

In order to test its performance, the Monte Carlo method was used to simulate the pdf transport equation for a model problem. The calculations reported here demonstrate the use of the method and are used to estimate the numerical error. The results show the following:

i) the Monte Carlo simulation converges to the solution of the differential equation,

ii) the expected value of the error is independent of N (*i.e.* the method is unbiased),

iii) the sampling error is proportional to $N^{-1/2}$, and

iv) the sampling error is independent of h.

4.1 *The Model Problem*

The model problem corresponds to a plug-flow reactor with imperfect mixing. The flow is one-dimensional with the uniform velocity U being in the $\bar{x}$-direction. The density ρ, the turbulent diffusion coefficient Γ_T and the turbulent frequency ω are also uniform. A single scalar ϕ represents the concentration of reaction products which is zero at the start of the reactor ($\phi = 0$ at $\bar{x} = 0$) and is everywhere bound by zero and unity ($0 \leqslant \phi \leqslant 1$). Two cases are considered: in the first—the linear case—the reaction rate of ϕ is a linear function of ϕ; in the second—the non-linear case—there is an Arrhenius reaction rate.

The velocity U and the length of the reactor L are used to define the following dimensionless quantities:

$$t^* \equiv t\,U/L, \qquad x \equiv \bar{x}/L,$$

$$\Gamma^* \equiv \Gamma_T/(\rho\,UL), \qquad \omega^* \equiv \omega\,L/U,$$

$$S^*(\psi) \equiv S(\psi)L/U$$

and

$$E^*(\psi; x, t) \equiv E(\psi; x, t)/\omega. \tag{4.1}$$

The pdf of $\phi(x, t^*)$ is $p(\psi; x, t^*)$. The pdf transport equation for the model problem is obtained from Eq. (2.8) and the above definitions:

$$\frac{\partial p}{\partial t^*}+\frac{\partial p}{\partial x}+\frac{\partial}{\partial \psi}(p\,S^*(\psi)) = \Gamma^*\frac{\partial^2 p}{\partial x^2}+\omega^* E^*. \tag{4.2}$$

The boundary conditions are

$$p(\psi; 0, t^*) = \delta(\psi), \tag{4.3}$$

and at $x=1$

$$\frac{\partial^2}{\partial x^2}p(\psi; x, t^*) = 0, \tag{4.4}$$

and the initial condition—corresponding to complete reaction—is

$$p(\psi;x,0) = \delta(1-\psi) \tag{4.5}$$

The normalized reaction rate for the linear case is

$$S^*(\psi) = a_1(1-\psi) \tag{4.6}$$

where a_1 is a constant. The main reason for considering this case is that there is an exact solution for the mean value $\langle\phi\rangle$ in the steady state:

$$\langle\phi\rangle = 1-\exp(-bx) \tag{4.7}$$

where

$$b = \tfrac{1}{2}\{(1+4a_1\Gamma^*)^{1/2}-1\}/\Gamma^*. \tag{4.8}$$

(In fact this solution satisfies the downstream boundary condition only approximately, but the effect of the discrepancy is unimportant.)

The Arrhenius expression used in the non-linear case is

$$S^*(\psi) = a_2\times 2183\,.\,\psi(1-\psi) \times\exp(-20/(1+3\psi)). \tag{4.9}$$

a_2 is a constant and the multiplier 2183 is chosen so that the maximum value of $S^*(\psi)$ is a_2.

The values of the constants are selected so that each of the four processes—convection, diffusion, reaction and mixing—are of approximately equal importance. The values are

$$a_1 = 3.,\ a_2 = 10.,\ \omega^* = 20.,\ \Gamma^* = 0.1. \tag{4.10}$$

In general, the Monte Carlo calculations reported below were performed with $N = 40$ and $h = 0.1$. The smallest possible time step was used which, for the given N and h, is $k = 0.0025$.

4.2 *The Linear Case*

All the results for the linear case are at $t^* = 2$, by which time the steady state has been reached. The mean $\langle\phi\rangle$ and standard deviation ϕ' are plotted against x on Figure 1. The dashed line is the exact solution Eq. (4.7) and the full circles are the ensemble average values $\hat{\phi}$. The expected value of $\hat{\phi}$ was estimated by taking the arithmetic mean of $\hat{\phi}$ over 25 similar calculations (the sole difference

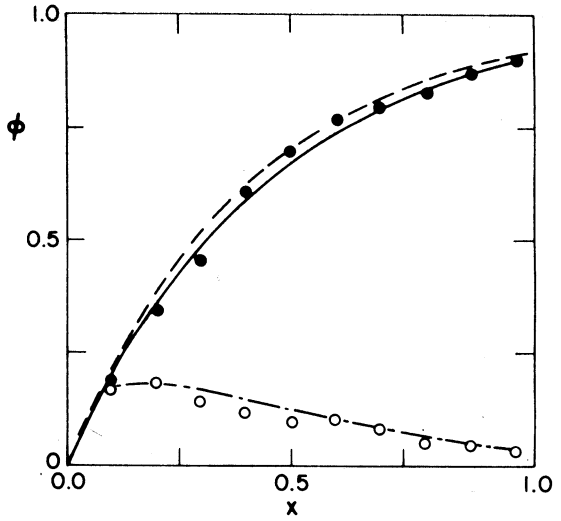

FIGURE 1 $\langle\phi\rangle$ and ϕ' against x: linear case, $N = 40$, $h = 0.1$; ---- $\langle\phi\rangle$, ——— $E\hat{\phi}$ and $\langle\phi\rangle_{fd}$, —·—· $E\phi'$, ● $\hat{\phi}$, ○ ϕ'.

between each calculation being the random numbers used). The expected value $E\hat{\phi}$ is shown as the solid line on the figure. Sampling error is evident from the differences between $\hat{\phi}$ and $E\hat{\phi}$.

According to the analysis of the previous section, as N tends to infinity, the Monte Carlo simulation converges to the finite-difference scheme given by Eqs. (3.22–3.25). Because the pdf equation is linear, the value of the mean given by the finite-difference equations $\langle\phi\rangle_{fd}$ can readily be computed. It is found that $\langle\phi\rangle_{fd}$ is equal to the expected value $E\hat{\phi}$. This observation provides strong evidence for the convergence and lack of bias in the method. As N tends to infinity, $\hat{\phi}$ tends to $E\hat{\phi}$ which is equal to $\langle\phi\rangle_{fd}$: as h tends to zero $\langle\phi\rangle_{fd}$ converges to the exact solution. Thus, as N and h^{-1} tend to infinity, $\hat{\phi}$ tends to the exact solution. The difference between the values of $\hat{\phi}$ and $E\hat{\phi}$ is sampling error due to finite N: the difference between $E\hat{\phi}$ and the exact solution is truncation error due to finite h^{-1}. The fact that $E\hat{\phi}$ is equal to $\langle\phi\rangle_{fd}$ for finite N ($N = 40$) strongly suggests that the method is unbiased.

The standard deviation ϕ' and its expected value are also shown on Figure 1. ϕ' reaches a maximum of almost 0.2 at $x = 0.2$ and then decays monotonically.

In order to study the dependence of the solution upon N, calculations were performed with values of N ranging from 10 to 400. Plotted against

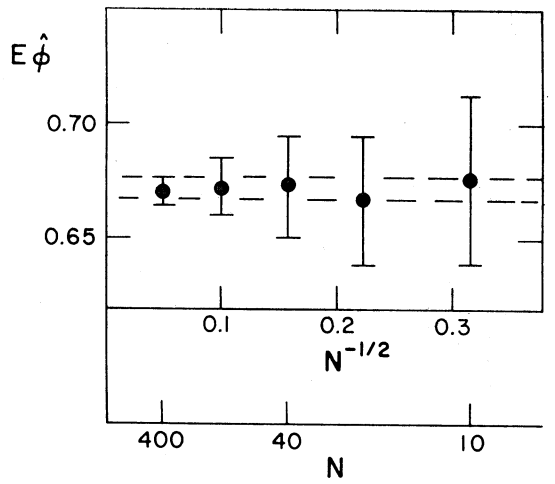

FIGURE 2 $E\hat{\phi} \pm \epsilon_{st}$ against $N^{-1/2}$: linear case, $x = 0.5$, $h = 0.1$.

$N^{-1/2}$ in Figure 2 is the expected value $E\hat{\phi}$ at $x = 0.5$ with error bars showing (twice) the standard error ϵ_{st},

$$\epsilon_{st}^2 = D\hat{\phi}. \tag{4.11}$$

The exact value of $E\hat{\phi}$ cannot be determined from a finite number of calculations: the dashed lines correspond to plus and minus one standard deviation uncertainty centered on the finite-difference solution $\langle\phi\rangle_{fd}$. The plot shows (to within the uncertainty of the test) that the expected value $E\hat{\phi}$ is equal to the finite-difference solution $\langle\phi\rangle_{fd}$ for all N. In other words, $\hat{\phi}$ is an unbiased estimate of $\langle\phi\rangle$. It may also be seen from the error bars that the standard error rises linearly with $N^{-1/2}$.

As h decreases, the amount of random sampling in the simulations of diffusion and convection increases. Tests were performed to determine if this leads to increased sampling error. Figure 3

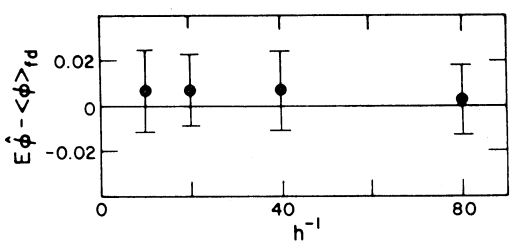

FIGURE 3 $E\hat{\phi} \pm \epsilon_{st} - \langle\phi\rangle_{fd}$ against h^{-1}: linear case, $x = 0.5$, $N = 40$.

shows the difference between $E\hat{\phi}$ and $\langle\phi\rangle_{fd}$ at $x = 0.5$ (with error bars showing the standard error) this time plotted against h^{-1}. It appears that the standard error is independent of h—a fortunate result.

In order to estimate the magnitude of the sampling error, the quantity

$$\epsilon^* = N^{1/2}\epsilon_{st}/\phi' \tag{4.12}$$

is plotted against x in Figure 4 for $N = 10$, 40 and 400. Although there is considerable scatter, it is clear that ϵ^* is of order unity: the maximum value is 1.4. Consequently, inverting Eq. (4.12), the standard error can be estimated from

$$\epsilon_{st} = \epsilon^*\phi' N^{-1/2}, \tag{4.13}$$

where (at least for this case) ϵ^* is of order unity.

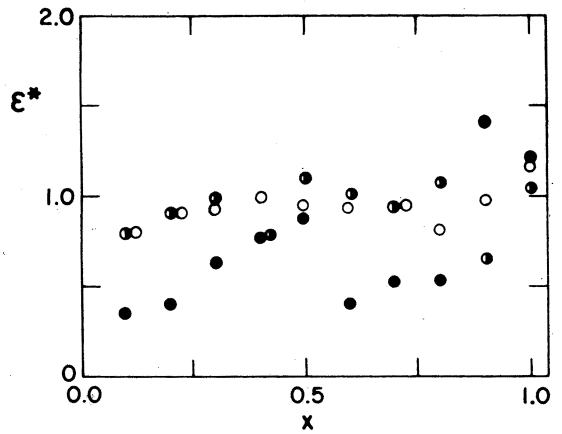

FIGURE 4 ϵ^* against x: linear case, $h = 0.1$. ○ N=10, ◑ $N = 40$, ● $N = 400$.

4.3 *The Non-linear Case*

A transient non-linear case was investigated to confirm the generality of the conclusions drawn from the steady-state linear case. In this series of tests the Arrhenius reaction rate was employed and the solution examined at times before the steady state had been reached.

The expected values $E\hat{\phi}$ are plotted against x in Figure 5 for the times $t^* = 0.5$, 1.0 and 1.5: the dashed line is the expected value of ϕ' and the circles are values of $\hat{\phi}$ at $t^* = 1.0$. It may be seen that the maximum value of ϕ' is about twice that of the linear case which accounts for the larger sampling error.

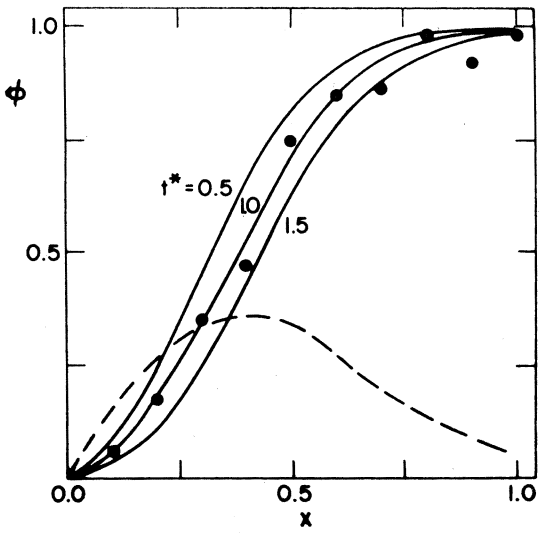

FIGURE 5. $\hat{\phi}$ and ϕ' against x: non-linear case, $N = 40$, $h = 0.1$. ——— $E\hat{\phi}$, ● $\hat{\phi}$ at $t^* = 1.0$, ---- $E\phi'$.

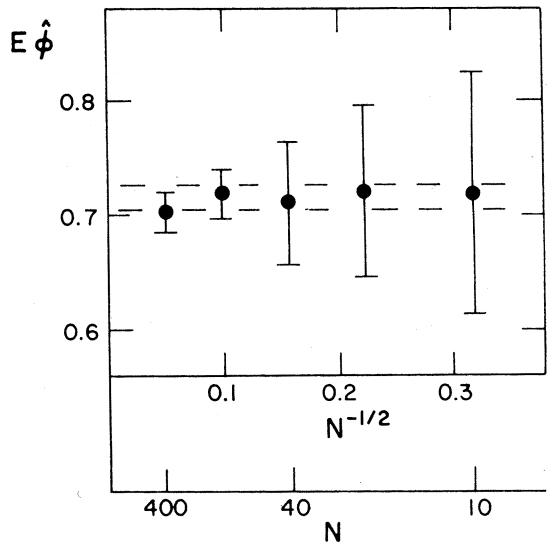

FIGURE 6 $E\hat{\phi} \pm \epsilon_{st}$ against $N^{-1/2}$: non-linear case, $\phi = 0.5$, $t^* = 1.0$, $h = 0.1$.

For $x = 0.5$ and $t^* = 1.0$, the expected value $E\hat{\phi}$ is plotted against $N^{-1/2}$ in Figure 6. The error bars show (twice) the standard error and, as in Figure 2, the dashed lines correspond to plus and minus one standard deviation uncertainty. Again, it appears that (to within the uncertainty of the test) $E\hat{\phi}$ is independent of N and the standard

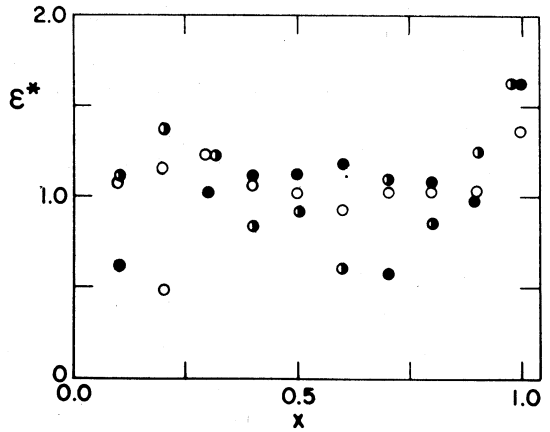

FIGURE 7 ϵ^* against x: non-linear case, $h = 0.1$. ○ $N = 10$, ◑ $N = 40$, ● $N = 400$.

error ϵ_{st} is proportional to $N^{-1/2}$. That $E\hat{\phi}$ is independent of N confirms the lack of bias in the method.

Figure 7 shows a plot of ϵ^* (see Eq. 4.12) against x for $N = 10$, 40 and 400. As in the linear case, there is a good deal of scatter but the mean value of ϵ^* is close to unity: the greatest value is 1.65.

In summary: test calculations for both a steady-state linear case and a transient non-linear case show that the Monte Carlo method is unbiased, and that the standard sampling error (of $\hat{\phi}$) is

$$\epsilon_{st} = \epsilon^* \phi' N^{-1/2}$$

where ϵ^* is of order unity and independent of h.

5. MIXING LAYER CALCULATIONS

The Monte Carlo method in conjunction with the $k-\epsilon$ turbulence model was used to calculate pdf's of temperature in a turbulent mixing layer. The results reported here show good agreement with the experimental data of Batt (1977). These data were obtained in a two-dimensional mixing layer in which the velocities of the two streams were 23 ft/s and 1.6 ft/s. The temperature difference between the streams was 5 °C.

In the calculations the slight density variation was ignored and, because of the nature of the flow, the boundary layer assumptions were invoked. The single scalar ϕ represents the normalized temperature ($\phi = 0$ in the high speed stream, $\phi = 1$ in the low speed stream). For this flow there is no heat source and hence $S(\phi)$ is zero. Thus, with U and V being the velocities in the x and y (flow and normal) directions, the transport equation for $p(\psi; x, y)$ is

$$U\frac{\partial p(\psi)}{\partial x} + V\frac{\partial p(\psi)}{\partial y} = \frac{\partial}{\partial y}\frac{\Gamma_T}{\rho}\frac{\partial p(\psi)}{\partial y} + E(\psi; x, y) \qquad (5.1)$$

Equations were also solved for the velocity U, the turbulent kinetic energy k and its rate of dissipation ϵ. These equations are:

$$\frac{\partial U}{\partial x} + \frac{\partial V}{\partial y} = 0, \qquad (5.2)$$

$$U\frac{\partial U}{\partial x} + V\frac{\partial U}{\partial y} = \frac{\partial}{\partial y}\nu_T\frac{\partial U}{\partial y}, \qquad (5.3)$$

$$U\frac{\partial k}{\partial x} + V\frac{\partial k}{\partial y} = \frac{\partial}{\partial y}\frac{\nu_T}{\sigma_k}\frac{\partial k}{\partial y} + \nu_T\left(\frac{\partial U}{\partial y}\right)^2 - \epsilon, \qquad (5.4)$$

and

$$U\frac{\partial \epsilon}{\partial x} + V\frac{\partial \epsilon}{\partial y} = \frac{\partial}{\partial y}\frac{\nu_T}{\sigma_\epsilon}\frac{\partial \epsilon}{\partial y} + C_{\epsilon 1}\frac{\nu_T \epsilon}{k}\left(\frac{\partial U}{\partial y}\right)^2 - C_{\epsilon 2}\epsilon^2/k, \qquad (5.5)$$

where the turbulent viscosity ν_T is given by

$$\nu_T = C_\mu k^2/\epsilon. \qquad (5.6)$$

The constants C_μ, $C_{\epsilon 1}$, $C_{\epsilon 2}$, σ_k and σ_ϵ are ascribed the standard values 0.09, 1.45, 1.9, 1.0, and 1.3.

It remains to specify Γ_T and ω in terms of k and ϵ. This is achieved by requiring that the pdf Eq. (5.1) be consistent with the standard model equation for $\langle \phi'^2 \rangle$ (Spalding, 1971). This yields,

$$\Gamma_T = \rho \nu_T / \sigma_\phi, \qquad (5.7)$$

and

$$\omega = 2C_\phi \epsilon / k, \qquad (5.8)$$

where the constants σ_ϕ and C_ϕ take the values 0.7 and 2.0.

Equations (5.2)–(5.6) were solved by a finite-difference procedure (Pope, 1977) with boundary and initial conditions appropriate to the mixing layer. The pdf equation was solved by a variant of

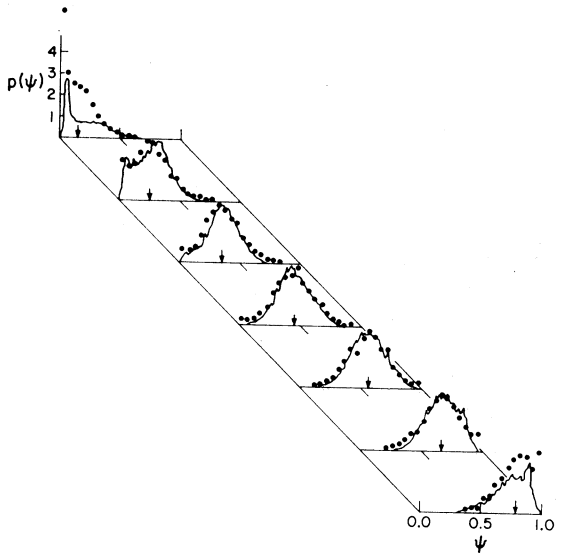

FIGURE 8 pdf's of temperature in a mixing layer: $p(\psi)$ against ψ (arrows show positions of means). ● Monte Carlo calculations, ~ Measurements of Batt (1977).

the Monte Carlo method which exploits the fact that Eq. (5.1) is parabolic. Rather than marching in time (as described in Section 3) the method marches in the downstream direction x. Thus initial ensembles are specified at $x = 0$ and each step of the simulation advances the ensembles a distance Δx downstream. In the cross-stream direction there were 24 nodes at each of which there was an ensemble of 100 elements. The step length Δx was very small—typically one-tenth of the mixing-layer thickness.

In order to make comparisons with measured pdf's, histograms (with 20 intervals) were constructed from the calculated ensembles. Figure 8 shows a comparison of these histograms with measured pdf's at seven cross-stream locations at $x = 15.5$ inches. It may be seen that in general the agreement is good: for the five central pdf's, the locations of the peaks† and the shapes and spreads of the distributions are closely matched. (The measurements at the extreme locations are suspect: in neither case does the pdf integrate to unity and, from similar data (*e.g.* Birch *et al.*, 1978), a spike resembling an exponential decay can be expected at the bounds $\psi = 0$ and $\psi = 1$.)

These calculations demonstrate the use of the Monte Carlo method and the good agreement with experimental data is encouraging considering the known shortcomings of some of the modelling assumptions.

† The comparisons between measured and calculated pdf's have been made where the mean values are the same. Consequently it is not surprising that the peaks nearly coincide.

6. DISCUSSION

Summary

A Monte Carlo method has been developed to solve the pdf equations of turbulent flow. At each node of a finite-difference grid covering the solution domain, the joint pdf is represented by an ensemble of N elements. Each element is ascribed a complete set of values of the relevant fluid properties. In a simulation of the scalar pdf Eq. (2.8), elements are commuted between neighbouring nodes (simulating diffusion) and they are transferred from node to node in the flow direction (simulating convection). Two elements mix by adopting the average values of their properties and, between mixing operations, the properties change according to the instantaneous reaction rates. The precise manner in which these operations are performed is determined in Section 3.

The performance of the method has been determined by analysis and by computational experiments. For large N, the tuncation error is proportional to the grid spacing h and the time step k. A finite value of N results in a random sampling error. The expected value of this error is zero (*i.e.* the method is unbiased) and the standard error is of order $N^{-1/2}$. From computational tests it appears that the standard sampling error (in determinging the mean $\langle\phi\rangle$) is

$$\epsilon_{st} = \epsilon^* \phi' N^{-1/2} \tag{6.1}$$

where ϵ^* is of order unity and independent of h.

The usefulness of the method stems from the fact that the computational work required increases only linearly with σ, the dimensionality of the joint pdf. Consequently, calculations of turbulent flows with many reactive species are possible.

The Monte Carlo method in conjunction with the $k-\epsilon$ turbulence model has been used to calculate pdf's of temperature in a mixing layer. The results agree well with the measurements of Batt (1977).

Computer Requirements

The method does not make great demands upon computer storage. At first sight, in order to perform a two-dimensional calculation on a 20×20 grid with 100 elements at each node, 40,000 storage locations per species would be required. This requirement would, on some computers, be prohibitive. However, the storage requirement can be reduced at will by splitting the calculation into several smaller calculations. Because the method is unbiased, the average of ten calculations with $N = 10$ has the same statistical error as one calculation with $N = 100$: the smaller calculations require the same computer time (altogether) but require only one tenth of the storage.

It has been shown in Section 3.6 that the computer time required is proportional to $N\sigma$: it is also approximately proportional to the number of nodes n. The mixing-layer calculations ($N = 100$, $n = 24$, $\sigma = 1$) were repeated four times in order to produce the required 4 percent accuracy for mean quantities. On a VAX 11 computer this required 4 minutes of CPU time. For the one-dimensional premixed flame calculations reported by Pope (1981a) ($N = 25$, $n = 20$, $\sigma = 3$), the calculations were repeated 30 times, again to produce 4 percent accuracy. The required CPU time was $2\frac{1}{2}$ minutes. It may be seen then that the method does not require unreasonable amounts of computer time and storage.

Relationship to Other Approaches

For homogeneous turbulence, where $p(\boldsymbol{\psi}; t)$ is independent of $\mathbf{x}$, the Monte Carlo method reduces to a simulation of reaction and mixing. Then the method differs only in detail from that of Spielman and Levenspiel (1965), which has subsequently been used by Flagan and Appleton (1974), Pratt (1976) and others. Indeed, the idea of the ensemble representation was taken from these works.

It has been known for some time that the Monte Carlo method in the form of random walks can be used to solve elliptic differential equations; Courant, Friedrichs and Lewy (1928). In these random walks, a "walker" passes from node to node of a finite-difference grid according to prescribed probabilities. At each node the value ascribed to the walker can be modified according to another prescription. Eventually the walker reaches the boundary of the solution domain where, we assume, the boundary value is specified. An estimate of the solution of the differential equation at the walker's point of origin can then be obtained from the boundary value and the final value of the walker. The accuracy of the result is improved by taking the average of the estimates obtained from many random walks.

Similarities between random walks and the present method are obvious. Minor differences are that, in the present method, an estimate of the solution is obtained over the whole field and that the walker's (element's) values originate from the boundary conditions. The major difference is that in the present method the walkers (elements) interact in the mixing process. For this reason ensembles of many elements are required rather than requiring a single walker to take many walks. Because of these differences the present analysis is completely different from that used for random walks.

Physical Interpretation

A physical interpretation of the Monte Carlo method is unnecessary and, in the author's opinion, should be avoided. It may be tempting to interpret a representative value $\boldsymbol{\varphi}^{(n)}$ as referring to the properties of a "particle" or "element of fluid". Since these "particles" conserve neither mass nor volume and since they can simply disappear, such an interpretation is likely to be misleading. Neither should the randomness of turbulence be seen reflected in the randomness of the Monte Carlo method. The method simulates a deterministic equation: random fluctuations in $\hat{\phi}$ are not due to turbulence but to sampling error (caused by finite N). Nor should the method be thought of as a physical model.

The physics is embodied in the pdf transport equation. The joint pdf is a well-defined, measurable quantity for which an exact transport equation can be derived. Modelling is applied to the exact equation in order to obtain Eq. (2.8), and the Monte Carlo method is no more than a numerical method for solving this equation.

Applications

The direct application of the method is to turbulent reactive flows. In spite of modelling uncertainties, the pdf equation most likely provides the best theoretical description (available at present) of such flows. Consequently, the Monte Carlo method is of direct practical value in enabling the solution of the equation, even when many species and complex kinetics are involved.

In recent years, many measurements have been made of pdf's and joint pdf's of velocity and a passive scalar in turbulent shear flows. Ribeiro and Whitelaw (1975) measured the joint pdf of velocity $p(v_1, v_2; \mathbf{x}, t)$ in a fully developed turbulent jet, and Wallace and Brodkey (1977) obtained similar measurements in a turbulent channel flow. For a heated turbulent jet, Venkataramini, Tutu and Chevray (1975) measured the joint pdf of velocity $p(v_1, v_2; \mathbf{x}, t)$ and also the joint pdf of velocity and temperature $p(\psi_1, v_1; \mathbf{x}, t)$. None of these data has been compared with theoretical calculations. Application of the Monte Carlo method to the transport equation for $p(\mathbf{v}, \boldsymbol{\psi}; \mathbf{x}, t)$ (see Pope, 1981b) would make such a comparison possible.

REFERENCES

Batt, R. G. (1977). Turbulent mixing in a low speed shear layer. *J. Fluid Mech.*, **82**, 53.

Birch, A. G., Brown, D. R., Dodson, M. G., and Thomas, J. R. (1978). The turbulent concentration field of a methane jet. *J. Fluid Mech.*, **88**, 431–449.

Courant, R., Freidrichs, K., and Lewy, H. (1928). Über die partiellen Differenzengleichungen der mathematischen Physik. *Math. Ann.*, **100**, 32.

Curl, R. L. (1963). Dispersed phase mixing: I. Theory and effects of simple reactors. *A.I.Ch.E.J.*, **9**, 175.

Dopazo, C. (1975). Probability density function approach for a turbulent axisymmetric heated jet: Centreline evolution. *Phys. Fluids*, **18**, 397.

Flagan, R. C., and Appleton, J. P. (1974). A stochastic model of turbulent mixing with chemical reaction: Nitric oxide formation in a plug-flow burner. *Combustion and Flame*, **23**, 249–267.

Gnedenko, B. V. (1962). *The Theory of Probability*, Chelsea, New York, p. 309.

Handscomb, D. C., and Hammersley, J. M. (1965). *Monte Carlo Methods*, Methuen, London.

Janicka, J., Kolbe, W., and Kollmann, W. (1979). Closure of the transport equation for the pdf of turbulent scalar fields. *J. Nonequil. Thermodyn.*, **4**, 47.

Janicka, J., Kolbe, W., and Kollmann, W. (1978). The solution of a PDF-transport equation for turbulent diffusion flames. *Proc. 1978 Heat Trans. Fluid Mech. Inst.*, Stanford University.

Lundgren, T. S. (1969). Model equation for nonhomogeneous turbulence. *Phys. Fluids*, **12**, 485.

Pope, S. B. (1976). The probability approach to the modelling of turbulent reacting flows. *Combustion and Flame*, **27**, 299.

Pope, S. B. (1977). A novel calculation procedure for free shear flows. Imperial College report FS/77/7.

Pope, S. B. (1979). The statistical theory of turbulent flames. *Phil. Trans. R. Soc. Lond.*, A, **291**, 529.

Pope, S. B. (1980). A Monte Carlo method for the pdf equations of turbulent flow. M.I.T. Report EL-80-012.

Pope, S. B. (1981a). Monte Carlo calculations of premixed turbulent flames. *Eighteenth Symposium (International) on Combustion*, the Combustion Institute.

Pope, S. B. (1981b). Transport equation for the joint pdf of velocity and scalars in turbulent flow. *Phys. Fluids*, to appear.

Pratt, D. T. (1976). Mixing and chemical reaction in continuous combustion. *Prog. Energy Combust. Sci.*, **1**, 73.

Ribeiro, M. M. (1976). The turbulence structure of free jet flows with and without swirl. Ph.D. thesis, University of London.

Ribeiro, M. M., and Whitelaw, J. H. (1975). Statistical characteristics of a turbulent jet. *J. Fluid Mech.*, **70**, 1.

Shreider, Yu. A. (Ed.) (1966). *The Monte Carlo Method*, Pergamon, London.

Spalding, D. B. (1971). Concentration fluctuations in a round turbulent free jet. *Chem. Eng. Sci.*, **26**, 95.

Spielman, L. A., and Levenspiel, O. (1965). A Monte Carlo treatment for reacting and coalescing dispersed phase systems. *Chem. Eng. Sci.*, **20**, 247.

Venkataramini, K. S., Tutu, N. K., and Chevray, R. (1975). Probability distributions in a round heated jet. *Phys. Fluids*, **18**, 1413.

Wallace, J. M., and Brodkey, R. S. (1977). Reynolds stress and joint probability distributions in the u–v plane of a turbulent channel flow. *Phys. Fluids*, **20**, 351.